Dynamics of the diode-pumped Kerr-lens mode-locked Nd:YAG laser

Alejandro A. Hnilo and Miguel A. Larotonda

Centro de Investigaciones en Laseres y Aplicaciones, Instituto de Investigaciones Científicas y Técnicas de las Fuerzas Armadas, Consejo Nacional de Investigaciones Científicas y Técnicas, Zufriategui 4380, (1603) Villa Martelli, Argentina

Received November 27, 2000; revised manuscript received April 2, 2001

We present a theoretical and experimental study of the dynamics of the diode-pumped Kerr-lens mode-locked Nd:YAG laser. The theoretical approach, which is based on a two-variable Poincaré map, allows the calculation of the pulse parameters with satisfactory accuracy. It is concluded (both theoretically and experimentally) that this laser does not present instabilities, which is an interesting feature for short-pulse laser engineering. We also find a robust two pulses per round trip mode of operation that appears to be a simple way for doubling the repetition rate. © 2001 Optical Society of America

OCIS codes: 140.4050, 140.3480, 190.1450, 190.3270, 140.1540.

1. INTRODUCTION

Kerr-lens mode-locked (KLM) lasers are not only a practical source of short and ultrashort light pulses, but also a nonlinear system of dynamical interest. The KLM Ti:sapphire laser has been the subject of much theoretical and experimental study. Quasi periodicity, multistability period-doubling cascades, tangent and period-three bifurcations, and chaos have been observed and described from different points of view.[1–4] In this paper we present the results of our study on the dynamics of the KLM Nd:YAG laser. This study is of interest because the Nd:YAG laser is, in a dynamical sense, complementary to the Ti:sapphire laser. In a Ti:sapphire the ultrashort-pulse-formation process is ruled by the balance of group-velocity-dispersion effects and the nonlinear self-amplitude and self-phase modulation effects. In Nd:YAG, instead, dispersion effects are negligible, and spatial-aperture-based effects are determinant. Besides, the former operates in the weak-saturation-gain regime, whereas the latter operates in the strongly saturated-gain regime.

The experimental part of this study is performed in a recently developed diode-pumped KLM Nd:YAG laser prototype.[5] The pump stability and repeatability allow reliable observation of the dynamical behavior. The theoretical part is based on iterative or Poincaré maps. This approach has been successfully demonstrated in Ti:sapphire, where a five-variable map is able to describe most of the observed dynamics.[6] In the case of Nd:YAG, a two-variable map suffices, as is explained in Section 2, where we compare theoretical predictions with observed results. In Section 3 we consider in some detail the case of a robust "instability" that is promising as a simple way of doubling the mode-locking repetition rate.

2. POINCARÉ MAP FOR THE KLM Nd:YAG LASER

The laser cavity is sketched in Fig. 1. It is described in detail in Ref. 5. For a cw pump power of 3 W (at 808 nm), the output is a train of (sech^2 shaped) 4.5-ps transform-limited pulses at a repetition of 101.5 MHz and 800-mW average power (at 1064 nm). The mode locking starts spontaneously; no external perturbation is needed (i.e., it is self-starting). The Kerr lens formed (at the passage of the laser pulse) in the high-nonlinear-index SF57 glass focuses the beam in the laser rod. In this way the losses at the aperture, formed by the pump-generated thermal-lens aberrations, are lower for pulsed operation than for cw operation.[7] This effect can be described by writing the round-trip Gaussian matrix and obtaining a recursive equation, linking the pulse-variable values at the $n + 1$ round trip with the values taken at the nth round trip. This leads naturally to a four-dimensional map where the variables are the pulse duration and chirp and the beam size and radius of curvature. A fifth equation (for the pulse energy) is obtained from the equation of gain saturation. This is the way the five-variable map for the Ti:sapphire laser is obtained.[8] In Ti:sapphire the ray and ray-pulse matrices have real elements (i.e., no imaginary parts), which means that no spatial apertures or bandwidth-limiting elements are included in the model. The simplification works well if one considers the stability against cw operation separately. But this simplification is impossible in Nd:YAG, where the KLM is of the pure-saturable-absorber type (i.e., determined by the spatial aperture). On the other hand, including matrices with complex elements in the five-dimensional approach used for Ti:sapphire leads to expressions that are almost impossible to handle.

Fortunately, in the case of Nd:YAG we have other simplifications at hand. The observed pulses are practically transform limited, and, because of their duration, they suffer negligible dispersion during one round trip. As a consequence, in a first approximation to the problem, the equation for the chirp can be disregarded. More importantly, the effect of the variation of the beam size and the radius of curvature can be taken into account in a compact way through the small-signal relative spot-size variation parameter[9] (note that we define it as positive):

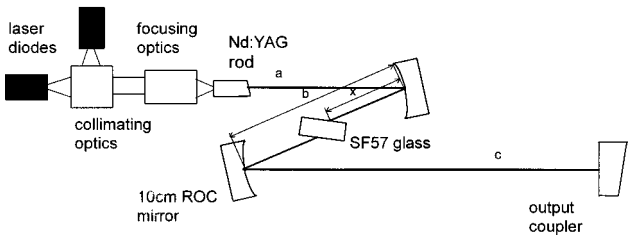

Fig. 1. Scheme of the laser cavity (from Ref. 5). The output coupler is wedged and has a transmission of 6%. The dimensions are $a = 343\,\mathrm{mm}$, $b = 104\,\mathrm{mm}$, $c = 1006\,\mathrm{mm}$, and $x = 56\,\mathrm{mm}$.

$$\delta \equiv -(1/w)\mathrm{d}w/\mathrm{d}P|_{P=0}, \tag{1}$$

where w is the beam radius and P is the pulse power. We refer to this δ parameter as the KLM strength, as it measures the ability of the cavity to perform a discrimination between the high-power (pulsed) and the low-power (continuous) regimes. In this way, three out of five variables become unnecessary for the description, as is described below. The map takes into account the effect of the peak-power sensitive aperture (nonlinear glass plus aperture) and the laser amplifier.

At this point we remark that an approach of this type is not meant to be a precise quantitative description of the KLM laser. A complex nonlinear system is sensitive to noise and fluctuations of the parameters, which makes a precise numerical prediction hopeless. Instead, our approach is meant to reveal the structurally stable properties of the system, such as the instabilities that appear if a given parameter is varied in a certain way. These properties depend on deeper topological properties of the dynamical system, which are presumably robust. Of course, in the cases that the approach does provide an adequate numerical estimation of the observable variables, we have a good reason to consider it reliable and potentially useful to help in laser design.

We assume that the electric field in the laser pulse has a Gaussian shape:

$$E(t) = E_0 \exp(-at^2 + i\omega_0 t), \tag{2}$$

where ω_0 is the carrier optical frequency, and $a = 2\ln 2/\tau^2$, where τ is the (intensity) FWHM pulse duration. As the pulse propagates into the cavity, it is affected by the spatial aperture, the amplifier's bandwidth (both in the laser rod), and the linear losses, mostly at the output coupler. The spatial aperture consists of the thermal-lens aberrations produced by the strong absorption of the pump light within a few millimeters of the Nd:YAG crystal. The transmission at the aperture is assumed:

$$T_{\mathrm{ap}}(t) \approx \exp - [w(t)/w_{\mathrm{ap}}]^2, \tag{3}$$

where w_{ap} is the equivalent radius of the aperture. The beam radius $w(t)$ is a function of time because it varies with the instantaneous value taken by the Kerr lens, which in turn is a function of the instantaneous pulse power $P(t)$. Therefore from Eq. (1),

$$T_{\mathrm{ap}}(t) = \exp\{-(w_{\mathrm{cw}}/w_{\mathrm{ap}})^2 \exp[-2\delta P(t)]\}. \tag{4}$$

We define the parameter $\mu \equiv (w_{\mathrm{cw}}/w_{\mathrm{ap}})^2$, which is the rate between the beam area (at cw) and the aperture area, and we define the variable $r \equiv 2\delta\mu P_p$, which is essentially the pulse's peak power scaled with the critical power (in the SF57 material, ~80 kW) and the KLM strength. The field $E'(t)$ after the aperture is found simply by multiplying input field (2) by transmission (4):

$$E'(t) = E_0 \exp\{-[1 + r\exp(-r/\mu)]at^2 + i\omega_0 t - \mu\exp(-r/\mu)\}, \tag{5}$$

where we approximate the pulse with a quadratic shape; $P(t) \approx P_p(1 - at^2)$, and assume that r is not much larger than 1. This is a reasonable assumption because the Kerr nonlinearity is usually a small perturbation.[7] The effect of the amplifier is well known,[10] so we merely transcribe the result:

$$1/(4a_{\mathrm{out}}) = 1/(4a_{\mathrm{in}}) + 4G/\Delta\omega^2, \tag{6}$$

$$E_{\mathrm{out}} = E_{\mathrm{in}}\exp(G), \tag{7}$$

where $\Delta\omega$ is the amplifier's bandwidth and G is the saturated single-passage gain. In Eq. (6), $a_{\mathrm{out}}(a_{\mathrm{in}})$ follows the notation of Eq. (2), and is proportional to the inverse of the square of the pulse width after (before) the gain medium. Similarly, E_{out} and E_{in} denote the amplitude of the field after and before crossing the gain medium. We now scale the variable a with the bandwidth ($\alpha \equiv a/\Delta\omega^2$), and we obtain the expressions that link the values of the variables (α, r) at the $n+1$ round trip with those at the nth round trip as

$$\alpha_{n+1} = \frac{\alpha_n[1 + r_n\exp(-r_n/\mu)]}{1 + 16G\alpha_n[1 + r_n\exp(-r_n/\mu)]}, \tag{8}$$

$$r_{n+1} = r_n\exp\{2[G - \mu\exp(-r_n/\mu) + \ln(k)]\}, \tag{9}$$

where k is the (field) round-trip feedback factor, which accounts for the linear losses. The value of G is obtained by recalling that gain saturation is strong in Nd:YAG and that it is produced in an averaged way over the mode-locking train; thus

$$G \approx g_{\mathrm{ss}}I_{\mathrm{sat}}/\langle I\rangle = g_{\mathrm{ss}}I_{\mathrm{sat}}\pi w^2\tau_{\mathrm{rt}}/U = g_{\mathrm{ss}}I_{\mathrm{sat}}\pi w_{\mathrm{cw}}^2\exp(-r/\mu)\tau_{\mathrm{rt}}/U, \tag{10}$$

where I_{sat} is the saturation intensity for Nd:YAG ($\approx$2.9 kW/cm^2), g_{ss} is the small-signal gain, τ_{rt} is the round-trip time, and $U = \tau P_p$ is the total pulse energy. This expression can be rewritten as

$$G = g(\alpha^{1/2}/r)\exp(-r/\mu), \tag{11}$$

where $g \equiv 2\pi(2\ln 2)^{-1/2}\delta\mu I_{\mathrm{sat}}w_{\mathrm{cw}}^2\tau_{\mathrm{rt}}\Delta\omega g_{\mathrm{ss}} \approx 8$, for typical values. Substituting Eq. (11) into Eqs. (8) and (9), we finally have the complete map:

$$\alpha_{n+1} = \frac{\alpha_n[1 + r_n\exp(-r_n/\mu)]}{1 + 16g\alpha_n^{3/2}\dfrac{\exp(-r_n/\mu)}{r_n}[1 + r_n\exp(-r_n/\mu)]}, \tag{12}$$

$$r_{n+1} = r_n\exp\{2[g(\alpha_n^{1/2}/r_n)\exp(-r_n/\mu) - \mu\exp(-r_n/\mu) + \ln(k)]\}. \tag{13}$$

The two variables, of the map, α_n and r_n, are related to the pulse duration and power. There are three control parameters: g, which is essentially related to the small-signal gain and the KLM strength; μ, which measures the overlap between the laser mode and the aperture; and k, which accounts for the linear losses. All of them are dimensionless.

3. COMPARISON WITH OBSERVATIONS

The fixed points α, r of map (12) and (13) are the observable values of the variables of the laser pulse. The value of α is obtained easily from r as

$$\alpha = \left\{ \frac{r^2}{16g[1 + r\exp(-r/\mu)]} \right\}^{2/3}, \tag{14}$$

and r is obtained by numerically solving the equation

$$\left(\left\{ \frac{g^2}{16r[1 + r\exp(-r/\mu)]} \right\}^{1/3} - \mu \right) \exp(-r/\mu) + \ln(k) = 0. \tag{15}$$

Assuming $g = 8$, $k = 0.95$ (which means a 10% energy loss per round trip) and $\mu = 1$, we obtain $r = 1.56$ and $\alpha = 0.06$. For $\delta = 3/P_{\text{critical}}$,[5] $P_p = 26$ kW, in excellent agreement with the measured value of 25 kW. For $\Delta\omega = 2\pi \times 120$ GHz, $\tau = 6$ ps, in acceptable agreement with the 4.8-ps duration of the Gaussian fit (which is the assumed pulse shape) to the observed autocorrelation ion.[5] The numerical agreement can be improved by fine tuning the values of the physical parameters, but we prefer using tabulated values. As we remarked before, the approach is not meant to obtain a precise quantitative agreement.

The variation trends of the fixed point with the control parameters are plotted in Fig. 2. In Fig. 2(a) the pulse power increases (almost linearly) with the gain parameter, as expected. The pulse duration decreases asymptotically to the minimum allowable by the amplifier's bandwidth. The variation with the overlap parameter μ [Fig. 2(b)] has an optimal value of the beam-aperture area rate, which is near $\mu = 0.8$ (for $g = 8$ and $k = 0.95$). This prediction agrees with the observation that a careful adjustment of pump focusing is critical to obtain mode locking. Finally [Fig. 2(c)], the pulse duration increases and power drops if the losses are increased, as expected. Naturally, the pulse power diverges at the physically unattainable point $k = 1$ (zero losses). We conclude that the approach is a reliable description of the system.

One of the main advantages of the map approach is that the stability of the solutions against small perturbations can be easily computed by solving the eigenvalues equation of the linearized map evaluated at the fixed point.[6,8] While the absolute value of one or more eigenvalues become equal to 1, the associated eigenvectors indicate the directions (in phase space) along which the fixed point loses stability. We indicate with dotted curves in Fig. 2 the region where the fixed points are unstable. In all cases the instability is related with one eigenvalue that becomes smaller than -1, and the associated eigenvector is practically collinear with the variable r. This means that we should expect to observe a period-doubling bifurcation in pulse power, with almost no variation in pulse duration. Instabilities of this type have been observed in KLM Ti:sapphire lasers.[3]

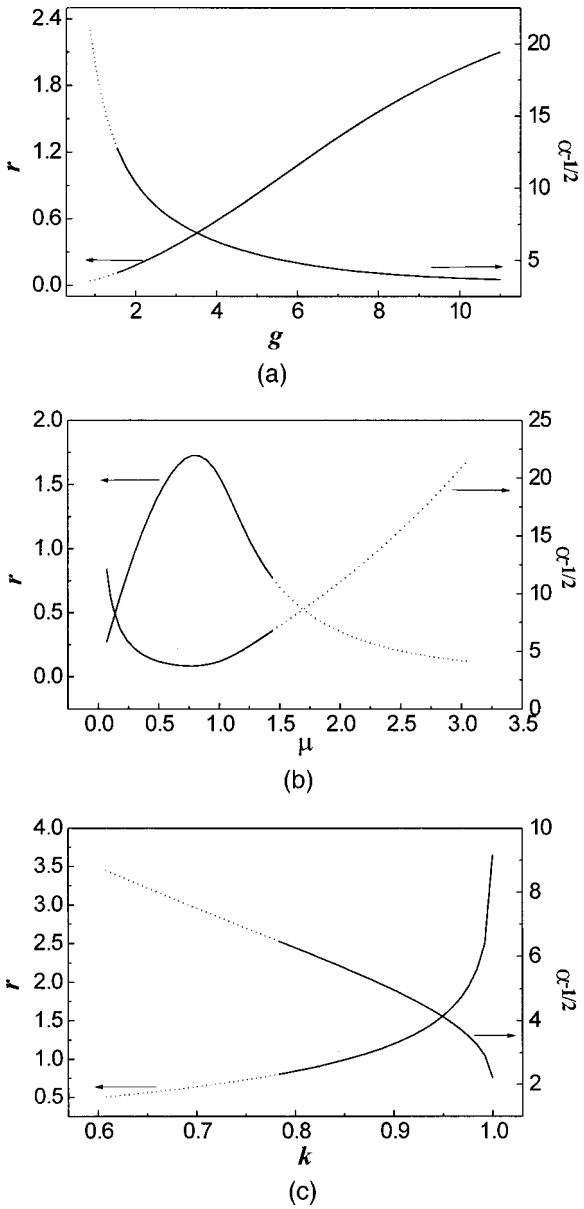

Fig. 2. Values of the fixed points as functions of the control parameters. The variable r is proportional to the pulse's peak power, and $\alpha^{-1/2}$ is proportional to the pulse duration. The dotted curves indicate that the fixed point is unstable in that region. (a) The gain parameter g varies for $k = 0.95$ and $\mu = 1$. (b) The beam-aperture overlap parameter μ varies for $g = 8$ and $k = 0.95$. (c) The field feedback factor k varies for $\mu = 1$ and $g = 8$.

However, no period doubling is observed in any position in parameter space. A closer look at the curves in Fig. 2 reveals that the unstable boundary merely reflects the laser threshold. The predicted period-doubling bifurcation is a kind of artifact caused by the assumption of strong saturation. Near the laser threshold the assumption fails, and hence the map [Eqs. (12) and (13)] is no longer a valid description. What really happens is that, as the gain/loss ratio decreases, the laser turns off. In the opposite direction (i.e., increasing gain) no instabilities are

predicted or observed in the range accessible to our setup. This is a good indication of the feasibility of scaling this laser's output by pumping with high-power stacks of diodes. The fact that a Nd:YAG mode-locked laser shows no anomalous behavior makes it an ideal source for high-power picosecond pulses.

Finally, we note from Fig. 2(b) that the mode-locked solution evolves in a stable way to the $r = 0 = \alpha$ limit (cw operation) as $\mu \to 0$ (no aperture), which means that the mode-locked solution is a continuous transformation of the cw solution. This explains why the bistability cw mode locking is not observed (as in Ti:sapphire).

4. TWO PULSES PER ROUND TRIP

During the scanning of the parameter values looking for bifurcations, we consistently find a two-pulse per round trip mode of operation that appears extremely robust. The pulses are of the same intensity, but unevenly separated by ~ 2.7 and ~ 7.3 ns from each other (see Fig. 3). The average output power and spectral and beam characteristics are the same as in the case of perfect mode-locking, but the autocorrelation is 1.3 times longer. The separation between pulses, and the figures and ratios of the perfect mode-locking regime, are observed to remain constant. We name this mode of operation P_2 (we name the perfect mode locking P_1). It coexists with P_1: mechanical noise induces transitions from one mode of operation to the other. But P_2 is less sensitive to misalignment or variations of the parameters, and it is observed stable for a broader parameter range than is P_1.

In mode P_2 the pulses induce a different KLM strength when crossing the SF57 glass rod in one direction or the other. In one direction the Kerr lens is induced by the propagating pulse alone (as in the P_1 mode). In the other direction each pulse finds the other going in the opposite direction, and both pulses cooperate to induce the Kerr lens. As the pulses are coherent, the KLM strength is four times larger when the pulses cooperate than when a single pulse traverses the rod. This is the reason why the two pulses are locked at 2.7 and 7.3 ns; these pulse separations correspond to the relative position of the SF57 rod inside the laser cavity (see Fig. 1). Any relative displacement of the pulses cancels the cooperative effect, and the total KLM strength becomes insufficient to sustain two pulses per round trip mode locking. If the SF57 rod were in the middle of the cavity, the two pulses would be equidistant, and they would cooperate with the KLM force in both directions of propagation. This mode of operation (which may be called the degenerate P_2 mode) is presumably the most robust cavity design for this type of laser. A similar multiple-pulse regime in a femtosecond KLM Ti:sapphire laser was reported by Lai *et al.*,[11] and its origin was attributed to an enhancement of the Kerr effect caused by the superposition of the two pulses in the nonlinear medium. According to Lai *et al.*, there is a narrow maximum of the KLM strength of the two pulses when they collide inside the Ti:sapphire rod, which sets the pulse separation tightly. A careful design that sets the cavity length to an exact multiple of the distance between the nonlinear glass and the gain–soft-aperture medium is thus a way to produce symmetric multipulse operation. A cavity that quadruples the repetition rate is currently under study.

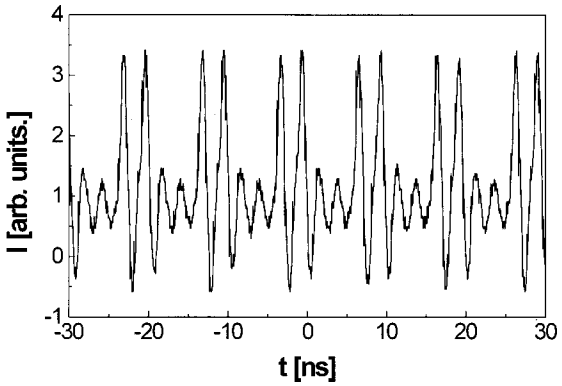

Fig. 3. Trace of the two pulses per round trip mode of operation (here named P_2), obtained with a fast photodiode (<0.3-ns rise time) and a 2-GSa/s sampling oscilloscope. The pulses have a duration (Gaussian fit) of 6.2 ps (not measurable with this method of observation). The small peaks between pulses are electrical echoes.

The KLM strength is measured by the parameter δ [Eq. (1)]. In the case that the KLM strength is different for each direction of propagation the total KLM strength is

$$\delta_{(P2)} = \delta_{(P1)}(z^+ + z^-)/2, \tag{16}$$

where $\delta_{(P1)}$ is the KLM strength for the mode P_i, and $z^+(z^-)$ is the rate between the KLM strength induced when the pulse propagates in the positive (negative) direction and the KLM strength induced in the mode P_1. Expression (16) is not as trivial as it may appear. It is not immediate that the total KLM strength is the mere sum of the going and the coming KLM strengths. Result (16) is obtained by computing $\delta_{(P2)}$ and $\delta_{(P1)}$ in an explicit way and comparing the final expressions.

Equation (16) allows us to estimate the pulse parameters in mode P_2. However, we warn that a complete description of P_2 is a different and much more difficult problem. An enlargement of the model needs the inclusion of other variables, such as the chirp and pulse bandwidth. The curve in Fig. 2 can be used to obtain a rough estimate of the pulse variables for this mode: as the total average power and beam characteristics are the same as in P_1, the pulse energy is about half than in P_1. Assuming that positive is the case of only one pulse in the rod, and taking into account the expression of the Kerr-lens focal length,[8] we have

$$z^+ = \frac{KU_{(P2)}/w_{(P2)}^4 \tau_{(P2)}}{KU_{(P1)}/w_{(P1)}^4 \tau_{(P1)}} = \frac{\tau_{(P1)}}{2\tau_{(P2)}}, \tag{17}$$

where K is proportional to the Kerr coefficient. As discussed above, $z^- = 4z^+$; thus

$$\delta_{(P2)} = \delta_{(P1)}(5/4)(\tau_{(P1)}/\tau_{(P2)}). \tag{18}$$

We assume now that the total KLM strength is roughly the same in both modes, and hence $\tau_{(P2)} \approx 1.25\tau_{(P1)}$, in satisfactory agreement with the measured value (=1.3). Regarding the pulse power, we note that the gain seen by each pulse in the mode P_2 is (on average) about one half of the gain seen by the single pulse in mode P_1; so $g_{(P2)}$

$= 8/2 = 4$, and then $r_{(P2)} = 0.6$ [see Fig. 2(a)]. This result agrees with the expected reduction in pulse power due to the halved pulse energy and the increase in the pulse duration ($2\times1.3=2.6=1.56/0.6$).

5. SUMMARY

We study, both theoretically and experimentally, the dynamics of the KLM Nd:YAG laser. We present a description in terms of a two-dimensional Poincaré map. This description is much simpler than the five-variable map that describes KLM Ti:sapphire lasers. This is possible thanks to the negligible intracavity dispersion of pulses in the 5-ps range and to the use of the parameter δ (the KLM strength). The description provides satisfactory estimations of the observed values of the pulse variables and a simple calculation of the regions of stability for perfect mode locking. It may be used as an auxiliary tool in the design of lasers of this kind.

In the experimental setup used, diode pumping provides steadiness and reproducibility to the observations. In agreement with the theoretical description, we conclude that the KLM Nd:YAG laser shows only the trivial threshold instability.

The only nontrivial mode of operation is the two pulses per round trip (P_2) mode. It seems to be even more robust than perfect mode locking, and it provides a simple way to double the repetition rate (which is of interest for many applications) of a given cavity, without affecting the beam characteristics nor the average power. However, a complete description of the dynamics of P_2 requires a significant enlargement of the theoretical approach presented here.

ACKNOWLEDGMENTS

This study was supported by Proyecto de Investigación Plurianual 425/98 and 639/98 of the Consejo Nacional de Investigaciones Científicas y Tecnológicas and by Proyecto de Investigación Científica y Tecnológica 1999-03-06303 of the Agencia Nacional de Promoción Científica y Tecnológica. Many thanks to Lic. M. Kovalsky for his help in the calculation of the eigenvectors.

REFERENCES

1. C. Wang, W. Zhang, K. Lee, and K. Yoo, "Pulse splitting in a self-mode-locked Ti:sapphire laser," Opt. Commun. **137**, 89–92 (1997).
2. S. Bolton, R. Jonks, C. Elkinton, and G. Sucha, "Pulse resolved measurements of subharmonic oscillations in a Kerr-lens mode-locked Ti:sapphire laser," J. Opt. Soc. Am. B **16**, 339–344 (1999).
3. M. Kovalsky, A. Hnilo, and C. González Inchauspe, "Hidden instabilities in the Ti:sapphire Kerr lens mode-locked laser," Opt. Lett. **24**, 1638–1940 (1999).
4. J. Jasapara, W. Rudolph, V. Kalashnikov, D. Krimer, J. Poloyko, and M. Lenzner, "Automodulations in Kerr-lens mode-locked solid-state lasers," J. Opt. Soc. Am. B **17**, 319–326 (2000).
5. M. Larotonda, A. Hnilo, and F. Diodati, "Diode-pumped self-starting Kerr-lens mode locking Nd:YAG laser," Opt. Commun. **183**, 485–491 (2000).
6. M. Kovalsky and A. Hnilo, "Stability and bifurcations in Kerr-lens mode-locked Ti:sapphire lasers," Opt. Commun. **186**, 155–166 (2000).
7. K. Liu, C. Flood, D. Walker, and H. van Driel, "Kerr lens mode locking of a diode pumped Nd:YAG laser," Opt. Lett. **17**, 1361–1363 (1992).
8. A. Hnilo, "Self-mode-locking Ti:sapphire laser description with an iterative map," J. Opt. Soc. Am. B **12**, 718–725 (1995).
9. G. Cerullo, S. De Silvestri, V. Magni, and L. Pallaro, "Resonators for Kerr-lens mode-locking femtosecond Ti:sapphire lasers," Opt. Lett. **19**, 807–809 (1994).
10. See, e.g., A. Siegman, *Lasers* (University Science, Mill Valley, Calif., 1986), Chap. 27.
11. M. Lai, J. Nicholson, and W. Rudolph, "Multiple pulse operation of a femtosecond Ti:sapphire laser," Opt. Commun. **142**, 45–49 (1997).